Radio Science, Volume 23, Number 5, Pages 791-808, September-October 1988

Intensity correlation function for waves of different frequencies propagating through a random medium

A. Bhattacharyya[1] and K. C. Yeh

Department of Electrical and Computer Engineering, University of Illinois, Urbana

(Received October 9, 1987; revised June 14, 1988; accepted June 15, 1988.)

The fourth-moment equation for plane waves of two different frequencies propagating through a two-dimensional, dispersive random medium, is solved numerically using a split step method. In this numerical scheme, the extended medium is replaced by a series of phase screens interspersed with diffraction layers and thus it provides a test for the validity of using a single effective phase screen to describe an extended random medium in the calculation of the intensity cross-correlation function. The intensity cross spectrum in the multiple scattering regime is calculated for different values of the ratio of the two frequencies under the "frozen flow" assumption, when temporal evolution of the irregularities is absent. Irregularities with either a Gaussian or a power law spectrum are considered. The effect of varying irregularity strength on the normalized cross correlation of intensity fluctuations observed at the same location is also investigated. The two-frequency intensity space-time cross-correlation function is determined for a special case of "nonfrozen" flow where the irregularities have a random drift superimposed on uniform convection.

1. INTRODUCTION

For a complete statistical description of a wave field after propagation through a random medium, it is necessary to calculate all the moments of the wave field with different transverse coordinates and different wave numbers. Equations which are satisfied by the moments of the complex amplitude of the wave field for different transverse coordinates and different wave numbers were derived by Lee [1974] under the forward scattering and Markov approximations. The Markov approximation is equivalent to the assumption that in the direction of propagation, the correlation scale of the random medium is much smaller than the correlation scale of the wave field. So far, solutions of the moment equations for waves of different frequencies have been restricted to the second moment [Liu and Yeh, 1975] and the fourth moment [Zavorotnyi, 1981; Mazar et al., 1985; Uscinski and Macaskill, 1985; Miller and Uscinski, 1986; Miller, 1987] under the "frozen field" approximation. In this approximation irregularities in the random medium convect with a uniform velocity. The two-frequency intensity space-time correlation function is of particular interest, since in many situations such as communication applications and interstellar scintillations of pulsar signals, the temporal and spatial evolution of the intensities of signals with different frequencies may be observed. Under the frozen field approximation, the spatial and temporal variation of the intensity cross-correlation function are simply related to each other through a linear translation due to the uniform convection of the irregularities. The two-frequency intensity correlation has been investigated analytically by Zavorotnyi [1981]. To make the mathematics tractable, he gives only asymptotic expressions under which the wave is assumed to satisfy the saturated statistics. Consistent with atmospheric applications, he also assumes the

[1] On leave from the Indian Institute of Geomagnetism, Bombay, India.

Paper number 88RS03079.
0048-6604/88/88RS-03079$08.00

background medium to be nondispersive and the dielectric fluctuations to have a Kolmogorov spectrum. Mazar et al. [1985] have used a two-scale expansion based on the smallness of a parameter, which does not depend on the scattering strength, to obtain a multidimensional integral expression for the two-frequency intensity correlation function in the case of a nondispersive medium with a Gaussian correlation function. The complexity of the higher order terms in their result restricts the intensity correlation functions to the zero-order term. Other analytic solutions of the fourth-moment equation for an extended random medium [Uscinski and Macaskill, 1985; Miller and Uscinski, 1986] also suffer from similar limitations. In these cases, expressions are obtained for the two-frequency intensity correlation function in the multiple scatter regime by approximately evaluating a multiple convolution solution of the relevant fourth-moment equation. Uscinski and Macaskill [1985] have considered both a plasma medium with a Gaussian irregularity spectrum which is characterized by a single scale size and a medium with a range of scale sizes corresponding to a power law irregularity spectrum. However, Miller and Uscinski [1986] have examined the range of validity of these results and have concluded that the approximations made in the evaluation of the multiple convolution solution lead to severe underestimation of the intensity cross spectrum at high spatial frequencies. Attempts at solving the fourth-moment equation numerically have been made by several investigators. The most thorough work is probably that given by Tur [1985]. He obtains numerical solutions for a Gaussian beam propagating in a two-dimensional nondispersive random medium with a Gaussian correlation function. However, he calculates these moments only for one single frequency. On the other hand, Miller [1987] has obtained analytic expressions for the intensity cross spectrum in the special case when the intensity fluctuations are caused by a one-dimensional deep phase screen with a randomly varying refractive index independent of the wave number and with a Gaussian spatial correlation function, and these compare well with the results of a direct numerical integration of the moment equation in this case.

In this paper, numerical solutions of the fourth-moment equation are obtained for waves of two different frequencies propagating through a two-dimensional extended medium with a wave number dependent refractive index, and in particular the characteristics of the intensity space-time cross correlation are investigated under both "frozen field" and nonfrozen conditions. Irregularities in the medium are considered to have either a Gaussian or a power law spectrum. The numerical scheme used to solve the fourth-moment equation is based on a split step algorithm which is an extension of a similar algorithm developed to solve a parabolic equation arising in the study of ocean acoustics [e.g., DiNapoli and Deavenport, 1979]. The method of solution of the fourth-moment equation for the general case of a space-time dependent correlation function for the refractive index of the medium is described in section 2. In section 3, numerical results for irregularities with a Gaussian spectrum under the "frozen flow" assumption are presented. The phase screen may be treated as a special case of the extended medium problem. For the propagation of monochromatic waves, the validity of using a single phase screen to describe an extended random medium has been examined by Booker et al. [1985]. For waves of different frequencies, however, not only does a phase screen give rise to different phase perturbations on the two waves, but also the diffraction which takes place after the waves emerge from a phase screen depends on the wave frequencies. Hence an extended random medium may not be adequately described by a single effective phase screen. This point is discussed with the help of some examples studied in section 3. In section 4, the nature of the spatial frequency cross spectrum of intensity fluctuations produced by irregularities with a power law spectrum under the frozen assumption is examined. The two-frequency intensity space-time correlation function for irregularities with either a Gaussian or a power law spectrum is described in section 5 for the situation where the irregularities have a random drift superimposed on uniform convection. Finally, this paper is concluded in section 6. Also discussed in this section is the relationship of the multiple convolution solution [Uscinski and Macaskill, 1985; Miller and Uscinski, 1986] with the numerical scheme used in this study.

2. NUMERICAL SOLUTION OF THE FOURTH MOMENT-EQUATION

2.1. The fourth-moment equation

For plane waves of unit amplitude propagating in the positive z direction and incident normally on a thick slab of irregularities extending from z = 0 to z = L, it is assumed that the refractive index of the slab does not vary in one of the transverse directions, so that it is only dependent on the two coordinates x and z. The frequency-, space-, and time-dependent complex amplitude u(x,z,t,k) for a wave field is defined in the usual manner by the relation

$$E(x,z,t,k) = u(x,z,t,k) \exp[-i(kz - \omega t)] \quad (1)$$

where k and ω are the wave number and angular frequency of the wave. The time scale τ for temporal variation of the irregularities in all physical situations is such that $\omega >> 2\pi/\tau$. Hence, under the forward scattering assumption, the complex amplitude u still satisfies the parabolic equation :

$$-2ik\frac{\partial u}{\partial z} + \frac{\partial^2 u}{\partial x^2} = -k^2 \varepsilon_1(x,z,t)u \quad (2)$$

where ε_1 represents the fluctuating part of the refractive index of the medium relative to the average refractive index. Here time t plays the role of a parameter which is introduced through the dependence of ε_1 on time. The derivation of the moment equations for different wave numbers by Lee [1974] starting from the parabolic equation (2) is therefore applicable.

In order to determine the two-frequency intensity space-time correlation function, it is necessary to solve the equation satisfied by the fourth moment

$$\Gamma_{2,2} = \langle u(x_1, z,t_1,k_1)\, u(x_2,z,t_2,k_2)\, u^*(x_3,z,t_1,k_1)\, u^*(x_4,z,t_2,k_2)\rangle \quad (3)$$

For propagation of radio waves in the ionosphere, the interplanetary space or the interstellar medium, the wave frequency ω satisfies the condition $\omega >> \omega_p$, the plasma frequency of the medium. Therefore $\varepsilon_1(x,z,t)$ is given by

$$\varepsilon_1(x,z,t) = -(\omega_p/\omega)^2\, \Delta N(x,z,t)/N_0 \quad (4)$$

where ΔN is the electron density fluctuation and N_0 is the background electron density. Then, following the derivation of Lee [1974], the fourth-moment equation satisfied by $\Gamma_{2,2}$ is

$$\begin{aligned}\frac{\partial}{\partial z}\Gamma_{2,2} = &-\frac{i}{2}\Big[\frac{1}{k_1}\Big(\frac{\partial^2}{\partial x_1^2} - \frac{\partial^2}{\partial x_3^2}\Big) + \frac{1}{k_2}\Big(\frac{\partial^2}{\partial x_2^2} - \frac{\partial^2}{\partial x_4^2}\Big)\Big]\Gamma_{2,2} - 4\pi^2 r_e^2 \\ &\cdot\Big\{\Big(\frac{1}{k_1^2} + \frac{1}{k_2^2}\Big) A_{\Delta N}(0,0) - \frac{1}{k_1^2} \cdot A_{\Delta N}(x_1 - x_3,0) - \frac{1}{k_2^2} A_{\Delta N}(x_2 - x_4,0) \\ &+ \frac{1}{k_1 k_2}\big[A_{\Delta N}(x_1 - x_2,t_1 - t_2) - A_{\Delta N}(x_1 - x_4,t_1 - t_2) - A_{\Delta N}(x_2 - x_3,t_2 - t_1) \\ &+ A_{\Delta N}(x_3 - x_4,t_1 - t_2)\big]\Big\}\Gamma_{2,2} \end{aligned} \quad (5)$$

where r_e is the classical electron radius and $A_{\Delta N}(x,t)$ is the integrated space-time correlation function for the electron density fluctuations :

$$A_{\Delta N}(x,t) = \int_{-\infty}^{\infty} B_{\Delta N}(x,z,t)\, dz \quad (6)$$

The occurrence of $A_{\Delta N}(x,t)$ in (5) is a consequence of the Markov approximation according to which the space-time correlation function of the density fluctuations is of the form

$$B_{\Delta N}(x,z,t) = A_{\Delta N}(x,t)\, \delta(z) \quad (7)$$

It will be seen later that $A_{\Delta N}(-x,-t) = A_{\Delta N}(x,t)$ even for the nonfrozen model of the irregularities.

With the introduction of the following coordinate transformation [Uscinski and Macaskill, 1985] and normalization with respect to a characteristic scale k_0^{-1} of the irregularities :

$$\begin{aligned} X &= \frac{k_0}{4}(x_1 + x_2 + x_3 + x_4) \\ x &= k_0[(x_1 - x_3) + \frac{1}{r}(x_2 - x_4)] \\ \xi_1 &= \frac{k_0}{2}[(x_1 + x_3) - (x_2 + x_4)] \\ \xi_2 &= \frac{k_0}{2}[(x_1 - x_3) - \frac{1}{r}(x_2 - x_4)] \end{aligned} \quad (8)$$

$$\zeta = k_0^2 z/k_1 \quad (9)$$

where $r = k_1/k_2$, (5) reduces to

$$\frac{\partial}{\partial \zeta}\Gamma_{2,2} = -i\frac{\partial^2}{\partial x \partial X}\Gamma_{2,2} - i\frac{\partial^2}{\partial \xi_1 \partial \xi_2}\Gamma_{2,2} - \frac{1}{2\zeta_L} F(x,\xi_1,\xi_2,t)\Gamma_{2,2} \quad (10)$$

where

$$t = t_1 - t_2 \quad \zeta_L = k_0^2 L/k_1$$

F does not depend on X because ΔN is assumed to be a homogeneous random field, and hence $\Gamma_{2,2}$ must be independent of X. Now x can be set equal to zero since the two-frequency intensity space-time correlation function is obtained from (3) by setting $x_3 = x_1$ and $x_4 = x_2$. Thus (10) further simplifies to

$$\frac{\partial}{\partial \zeta}\Gamma_{2,2} = -i\frac{\partial^2}{\partial \xi_1 \partial \xi_2}\Gamma_{2,2} - \frac{1}{2\zeta_L}F(\xi_1,\xi_2,t)\Gamma_{2,2} \qquad (11)$$

where

$$\begin{aligned}\frac{1}{2\zeta_L}F(\xi_1,\xi_2,t) = \frac{4\pi^2 r_e^2}{k_1 k_0^2}\{&(1+r^2)A_{\Delta N}(0,0)\\ &- A_{\Delta N}(\xi_2,0) - r^2 A_{\Delta N}(r\,\xi_2,0)\\ &+ r\,[A_{\Delta N}(\xi_1 + \tfrac{1+r}{2}\xi_2,t)\\ &- A_{\Delta N}(\xi_1 + \tfrac{1-r}{2}\xi_2,t)\\ &- A_{\Delta N}(\xi_1 - \tfrac{1-r}{2}\xi_2,t)\\ &+ A_{\Delta N}(\xi_1 - \tfrac{1+r}{2}\xi_2,t)]\}\end{aligned} \qquad (12)$$

2.2. Split step algorithm

Equation (11) may be written as

$$\frac{\partial}{\partial \zeta}\Gamma_{2,2} = i\,(C + D)\,\Gamma_{2,2} \qquad (13)$$

where the operators C and D are given by

$$C \equiv \frac{i}{2\zeta_L}F(\xi_1,\xi_2,t)$$
$$D \equiv -\frac{\partial^2}{\partial \xi_1 \partial \xi_2} \qquad (14)$$

The starting point for the split step algorithm is the assumption that the solution for $\Gamma_{2,2}$ at $\zeta_{n+1} = \zeta_n + \Delta\zeta(\Delta\zeta < 1)$ can be obtained from the solution at ζ_n according to

$$\Gamma_{2,2}(\zeta_{n+1},\xi_1,\xi_2,t) = e^{i\Delta\zeta(C+D)} \cdot \Gamma_{2,2}(\zeta_n,\xi_1,\xi_2,t) \qquad (15)$$

which is an exact solution only when the operators C and D commute with each other. The exponential operator which appears in (15) can be split up in various ways [e.g., DiNapoli and Deavenport, 1979]. The following approximation for the solution

$$\Gamma_{2,2}(\zeta_{n+1},\xi_1,\xi_2,t) = e^{i\Delta\zeta D/2} \cdot e^{i\Delta\zeta C} e^{i\Delta\zeta D/2}\,\Gamma_{2,2}(\zeta_n,\xi_1,\xi_2,t) \qquad (16)$$

is more accurate than the approximation

$$\Gamma_{2,2}(\zeta_{n+1},\xi_1,\xi_2,t) = e^{i\Delta\zeta D} e^{i\Delta\zeta C}\,\Gamma_{2,2}(\zeta_n,\xi_1,\xi_2,t) \qquad (17)$$

This can be seen by computing $\partial\Gamma_{2,2}/\partial\zeta$ using either (16) or (17) and comparing with the right-hand side of (13). Whereas the error involved in the approximation (16) is proportional to $(\Delta\zeta)^2$, that for approximation (17) is proportional to $\Delta\zeta$. Taking note of the fact that the operator C gives rise to phase perturbations due to the presence of the irregularities and the operator D gives rise to diffraction effects, the split step solution is seen to be equivalent to the replacement of the extended random medium by a series of phase screens and diffraction layers. Each phase screen imposes a phase perturbation equivalent to that produced by an irregularity slab of normalized thickness $\Delta\zeta$. Between two neighboring phase screens only diffraction or propagation effects take place. Such a phase screen - diffraction layer method has been used to solve the parabolic equation satisfied by the complex amplitude of a wave reflected from a turbulent ionosphere [Wagen and Yeh, 1986]. Earlier, recurrence relations for the complex field moments of arbitrary order were derived by Rino [1978] by iterative application of weak scatter theory, which was also based on the concept of successive phase screens and diffraction layers. The approximation considered in (16) is equivalent to placing the phase screens in the middle of each slab of thickness $\Delta\zeta$ as opposed to the top of each slab which corresponds to the situation described by (17).

With the introduction of

$$\Gamma'_{2,2}(\zeta_n,\xi_1,\xi_2,t) = e^{i\Delta\zeta D/2}\,\Gamma_{2,2}(\zeta_n,\xi_1,\xi_2,t) \quad (18)$$

it follows from (16) that

$$\Gamma'_{2,2}(\zeta_{n+1},\xi_1,\xi_2,t) = e^{i\Delta\zeta D} e^{i\Delta\zeta C} \cdot \Gamma'_{2,2}(\zeta_n,\xi_1,\xi_2,t) \quad (19)$$

To obtain the split step algorithm, let

$$V_2(\zeta_n,\xi_1,\xi_2,t) = e^{i\Delta\zeta C}\,\Gamma'_{2,2}(\zeta_n,\xi_1,\xi_2,t) \quad (20)$$

and its Fourier transform be denoted by $G_2(\zeta_n, q_1,q_2,t)$. Then

$$\Gamma'_{2,2}(\zeta_{n+1},\xi_1,\xi_2,t) = \int_{-\infty}^{\infty}\!\!\int G_2(\zeta_n,q_1,q_2,t) \cdot\exp(i\Delta\zeta q_1 q_2)\exp(iq_1\xi_1 + iq_2\xi_2)\,dq_1\,dq_2 \quad (21)$$

yields the value of $\Gamma'_{2,2}$ for the next step.

The split step method of solving the fourth-moment equation therefore involves computation of the Fourier transform G_2 of V_2 at each step followed by the evaluation of the inverse Fourier transform indicated in (21) to obtain a new value of $\Gamma'_{2,2}$ for the next step. It is to be noted that as $|\xi_1|$ or $|\xi_2| \to \infty$, $\partial^2\Gamma_{2,2}/\partial\xi_1\partial\xi_2 \to 0$. Also at $\zeta = 0$, $\Gamma_{2,2}(0, \xi_1, \xi_2, t) = 1$. Thus the moment equation (11) yields the following solutions under these conditions:

$$\Gamma_{2,2}(\zeta,|\xi_1|\to\infty,\xi_2,t) = \exp[-\frac{\zeta}{2\zeta_L}F(|\xi_1|\to\infty,\xi_2,t)]$$

$$\Gamma_{2,2}(\zeta,\xi_1,|\xi_2|\to\infty,t) = \exp[-\frac{\zeta}{2\zeta_L}F(\xi_1,|\xi_2|\to\infty,t)] \quad (22)$$

The corresponding values of $V_2(\zeta,\xi_1,\xi_2,t)$ for $|\xi_1| \to \infty$ or $|\xi_2| \to \infty$ can be derived from these solutions using (18) and (20). Before the application of discrete Fourier transform methods to obtain the required Fourier transforms at each step, V_2 is cast in the form

$$\begin{aligned} V_2(\zeta_n,\xi_1,\xi_2,t) &= v_2(\zeta_n,\xi_1,\xi_2,t) \\ &+ V_2(\zeta_n,|\xi_1|\to\infty,\xi_2,t) \\ &+ V_2(\zeta_n,\xi_1,|\xi_2|\to\infty,t) \\ &- V_2(\zeta_n,|\xi_1|\to\infty,|\xi_2|\to\infty,t) \end{aligned} \quad (23)$$

where $v_2(\zeta_n,\xi_1,\xi_2,t) \to 0$ for $|\xi_1|$ or $|\xi_2| \to \infty$, and the other terms on the right-hand side of (23) are determined by the boundary conditions on V_2. Thus the initial value of v_2 at $\zeta=0$ is

$$\begin{aligned} v_2(0,\xi_1,\xi_2,t) &= \exp[-\frac{\Delta\zeta}{2\zeta_L}F(\xi_1,\xi_2,t)] \\ &- \exp[-\frac{\Delta\zeta}{2\zeta_L}F(|\xi_1|\to\infty,\xi_2,t)] \\ &- \exp[-\frac{\Delta\zeta}{2\zeta_L}F(\xi_1,|\xi_2|\to\infty,t)] \\ &+ \exp[-\frac{\Delta\zeta}{2\zeta_L}F(|\xi_1|\to\infty,|\xi_2|\to\infty,t)] \end{aligned} \quad (24)$$

Next let $g_2(\zeta_n,q_1,q_2,t) = \Im[v_2(\zeta_n,\xi_1,\xi_2,t)]$ where $\Im$ indicates the Fourier transform. Then, using (20) and (21) it is straightforward to see that for the (n+1) th step,

$$\begin{aligned} v_2(\zeta_{n+1},\xi_1,\xi_2,t) &= \exp(i\Delta\zeta C) \\ &\cdot\Im^{-1}[\exp(i\Delta\zeta q_1 q_2)\, g_2(\zeta_n,q_1,q_2,t)] \\ &+ \exp(i\Delta\zeta C)\,\{V_2(\zeta_n,|\xi_1|\to\infty,\xi_2,t) \\ &+ V_2(\zeta_n,\xi_1,|\xi_2|\to\infty,t) \\ &- V_2(\zeta_n,|\xi_1|\to\infty,|\xi_2|\to\infty,t)\} \\ &- V_2(\zeta_{n+1},|\xi_1|\to\infty,\xi_2,t) \\ &- V_2(\zeta_{n+1},\xi_1,|\xi_2|\to\infty,t) \\ &+ V_2(\zeta_{n+1},|\xi_1|\to\infty,|\xi_2|\to\infty,t) \end{aligned} \quad (25)$$

The Fourier transform g_2 of v_2 and the inverse Fourier transform indicated by $\mathfrak{I}^{-1}$ in (25) can now be evaluated using a fast Fourier transform (FFT) algorithm. In this scheme of computation the constraints on $\Gamma_{2,2}$ described by (22) are automatically satisfied.

For the final step within the irregularity slab, (18), (19) and (20) yield

$$\Gamma_{2,2}(\zeta_L,\xi_1,\xi_2,t) = e^{i\Delta\zeta D/2} V_2(\zeta_L - \Delta\zeta,\xi_1,\xi_2,t) \tag{26}$$

In many of the physical situations where this formalism is applicable, there is further propagation of the waves beyond the irregularity slab. In this region, the operator C vanishes identically and $\Gamma_{2,2}$ satisfies the equation

$$\frac{\partial}{\partial\zeta}\Gamma_{2,2} = iD\Gamma_{2,2} \tag{27}$$

Thus the solution for $\Gamma_{2,2}$ at the receiver location ($\zeta = \zeta_R$) is

$$\Gamma_{2,2}(\zeta_R,\xi_1,\xi_2,t) = \exp[i(\zeta_R - \zeta_L)D] \cdot\Gamma_{2,2}(\zeta_L,\xi_1,\xi_2,t) \tag{28}$$

which on using (26) reduces to

$$\begin{aligned}\Gamma_{2,2}(\zeta_R,\xi_1,\xi_2,t) &= \exp[-\frac{1}{2}F(|\xi_1|\to\infty,\xi_2,t)] \\ &+ \exp[-\frac{1}{2}F(\xi_1,|\xi_2|\to\infty,t)] \\ &- \exp[-\frac{1}{2}F(|\xi_1|\to\infty,|\xi_2|\to\infty,t)] \\ &+ \mathfrak{I}^{-1}\{\exp[i(\zeta_R - \zeta_L + \frac{\Delta\zeta}{2})q_1q_2] \\ &\cdot g_2(\zeta_L - \Delta\zeta,q_1,q_2,t)\}\end{aligned} \tag{29}$$

2.3. Two-frequency intensity space-time correlation function

The space-time cross-correlation function of intensity fluctuations is defined as

$$R(\xi,t) = \frac{\langle I_1I_2\rangle - \langle I_1\rangle\langle I_2\rangle}{\langle I_1\rangle\langle I_2\rangle} \tag{30}$$

where

$$\begin{aligned} I_j &= u(x_j,z,t_j,k_j)\, u^*(x_j,z,t_j,k_j) \\ \xi &= k_0(x_1 - x_2) \\ t &= t_1 - t_2 \end{aligned}$$

Since $\langle I_1\rangle = \langle I_2\rangle = 1$ and $\langle I_1I_2\rangle$ can be obtained by taking $x_3 = x_1$ and $x_4 = x_2$ in (3), $R(\xi,t)$ is given by

$$R(\xi,t) = \Gamma_{2,2}(\zeta_R,\xi,0,t) - 1 \tag{31}$$

Furthermore, on the basis of differential equation (11), the existence of an integral constraint on $\Gamma_{2,2}(\zeta,\xi,0,t)$ can be demonstrated [Lerche, 1979]. This constraint requires that at each step, $\Gamma_{2,2}(\zeta,\xi,0,t)$ must satisfy the condition

$$\int_{-\infty}^{\infty} [\Gamma_{2,2}(\zeta,\xi,0,t) - 1]\, d\xi = 0 \tag{32}$$

and thus provides a test for the accuracy of the numerical solution.

3. GAUSSIAN IRREGULARITY SPECTRUM

In this section the random medium is considered to be frozen, such that

$$B_{\Delta N}(\vec{\rho},t) = B_{\Delta N}(\vec{\rho} - \vec{v}_0 t) \tag{33}$$

where $\vec{\rho}$ refers to the x-z coordinates and $\vec{v}_0$ is the uniform convection velocity of the irregularities in the medium. Thus it is not necessary to consider the time variation explicitly. Then the x-dependent integrated correlation function $A_{\Delta N}$ is related to the power spectrum of the irregularities through [Yeh and Liu, 1982]

$$A_{\Delta N}(x) = 2\pi \int_{-\infty}^{\infty} \Phi_{\Delta N}(q_x,0) \exp(iq_x x)\, dq_x \tag{34}$$

An irregularity power spectrum of the Gaussian form:

$$\Phi_{\Delta N}(\vec{q}) = [\langle(\Delta N)^2\rangle/\pi k_0^2] \exp(-q^2/k_0^2) \tag{35}$$

is frequently assumed for reasons of mathematical simplicity. For a Gaussian power spectrum, the function $F(\xi_1,\xi_2,t)$, which does not depend on t for the frozen case under consideration, is given by

$$\begin{aligned} F(\xi_1,\xi_2) = 2\sigma_\phi^2\{ & 1 + r^2 - \exp(-\xi_2^2/4) \\ & - r^2 \exp(-r^2\xi_2^2/4) \\ & + r(\exp[-(\xi_1 + \tfrac{1+r}{2}\xi_2)^2/4] \\ & - \exp[-(\xi_1 + \tfrac{1-r}{2}\xi_2)^2/4] \\ & - \exp[-(\xi_1 - \tfrac{1-r}{2}\xi_2)^2/4] \\ & + \exp[-(\xi_1 - \tfrac{1+r}{2}\xi_2)^2/4])\} \end{aligned} \qquad (36)$$

where σ_ϕ^2 is the variance of phase fluctuations produced by the random medium for waves with wave number k_1. It can be seen from (36) that $F(|\xi_1| \to \infty, 0) = 0$. Hence, according to (29) and (31), the two-frequency spatial correlation function for intensity fluctuations is of the form

$$\begin{aligned} R(\xi_1) = & \exp[-\tfrac{1}{2}F(\xi_1,|\xi_2| \to \infty)] \\ & - \exp[-\tfrac{1}{2}F(|\xi_1| \to \infty,|\xi_2| \to \infty)] \\ & + \Im^{-1}\{\exp[i(\zeta_R - \zeta_L + \tfrac{\Delta\zeta}{2})q_1q_2] \\ & \cdot g_2(\zeta_L - \Delta\zeta,q_1,q_2)\}|_{\xi_2=0} \end{aligned} \qquad (37)$$

The frequency cross spectrum of intensity fluctuations is then obtained from

$$P(\nu) = \frac{1}{2\pi}\int_{-\infty}^{\infty} R(\xi)\, e^{-i\xi}\, d\xi \qquad (38)$$

It should be noted that in the split step algorithm if the number of steps inside the random medium is reduced to one, the results obtained are those for an effective phase screen which replaces the extended random medium. This effective phase screen is located at the center of the thick slab, i.e., at $\zeta = \zeta_L/2$. For monochromatic waves, numerical solutions of the fourth-moment equation show that the intensity autocorrelation function for an extended medium is very well approximated by that for a centrally located phase screen which produces the same mean square fluctuation of phase σ_ϕ^2, as long as the Fresnel scale is smaller than the outer scale of the irregularities [Booker et al., 1985]. However, the situation is different for the intensity cross correlation of waves of different frequencies. In this case, as noted in section 1, it may be necessary to take into account the fact that the diffraction which takes place in the region between two successive phase screens depends on the wave frequency. In the fourth-moment equation (11), the diffraction effects which can be attributed to the difference in the frequencies of the two waves are manifested only through the r-dependent arguments of the integrated correlation functions $A_{\Delta N}$ which appear in $F(\xi_1,\xi_2,t)$, as a result of the coordinate transformations (8).

The discrepancy between the phase screen and extended medium results for the intensity cross-correlation function $R(\xi)$ is expected to be more pronounced as the thickness of the irregularity slab increases. Some results for a normalized thickness $\zeta_L = 0.38$ are shown in Figure 1. In terms of the irregularity scale size L_0 (= $2/k_0$), this thickness is $5 \times 10^2 L_0$. In order to allow for propagation outside the irregularity slab, ζ_R has been chosen such that $\zeta_R - \zeta_L = 0.13$. In this case, the effective phase screen would be located at a normalized distance $\zeta = 0.32$ from the receiver. The value of σ_ϕ^2 is 100 and the ratio of the two frequencies, $r = 0.714$. For the evaluation of $R(\xi)$ in the extended medium case, the step size in the split step algorithm has been taken as $\Delta\zeta = \zeta_L/4$. Decreasing the step size further did not produce appreciably different results as will be seen in Figure 2. In Figure 1, the intensity cross-correlation function $R(\xi)$ is shown as a function of the normalized distance ξ, for an extended medium and a centrally located phase screen. Thus replacement of the extended medium by an effective phase screen reduces the value of the two-frequency cross correlation of intensity fluctuations observed at a single location by as much as 33% in this case. The cross spectra $P(\nu)$ of intensity fluctuations computed with the step sizes $\Delta\zeta = \zeta_L$, $\Delta\zeta = \zeta_L/4$, and $\Delta\zeta = \zeta_L/10$ are plotted in Figure 2. In each case the computed value of $P(0)$ is less than 10^{-15} which, according to the constraint represented by (32), shows that the computation scheme yields fairly accurate results. The curves for $\Delta\zeta = \zeta_L/4$ and $\Delta\zeta = \zeta_L/10$ overlap for the spatial frequency range shown, but the phase screen yields lower values for the power

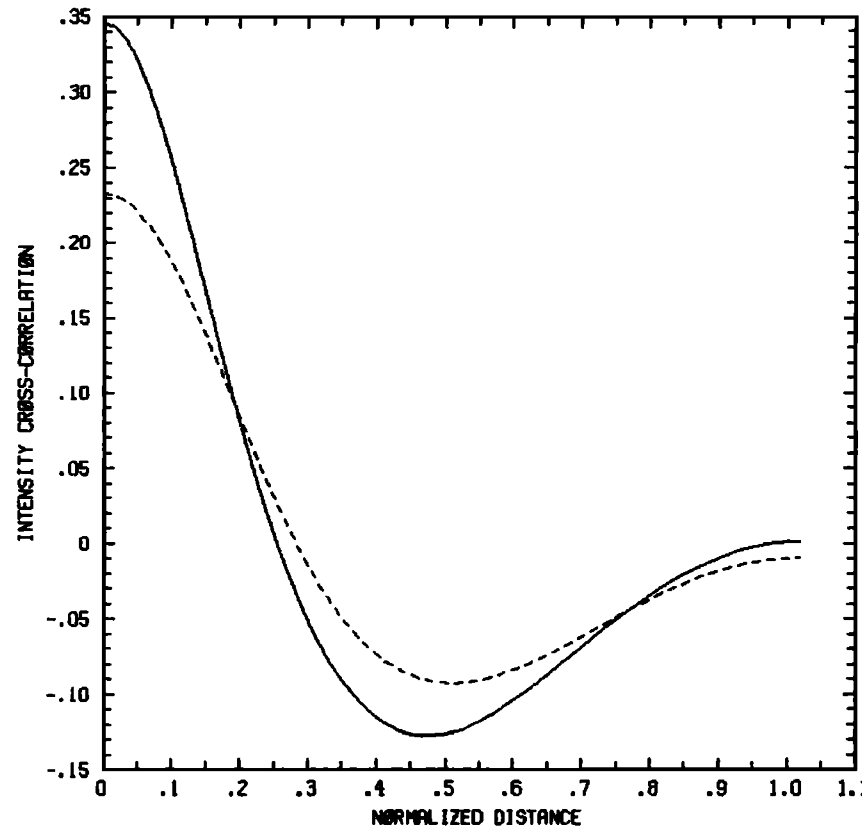

Fig. 1. Intensity cross-correlation functions for an irregularity slab of normalized thickness ζ_L = 0.38 (solid line), and a centrally located phase screen (dashed line). Irregularities have a Gaussian power spectrum with σ_ϕ^2 = 100. Ratio of the two frequencies, r, is 0.714.

spectrum over the entire range of spatial frequencies with a more rapid decrease in power at high spatial frequencies compared to that obtained for an extended medium.

Behavior of the two-frequency intensity cross spectrum at high spatial frequencies changes noticeably with r, the ratio of the two frequencies. For the purpose of comparison with the results obtained by Miller [1987] (see in particular, Figure 4 of this reference), the phase screen results for three values of r, namely r = 1, 0.714, and 0.5, are presented in Figure 3. Due to the limitation of frequency resolution in the present calculation, values of the intensity cross spectrum at spatial frequencies ν lying between 0 and the lowest frequency depicted in Figure 3 are unavailable. This problem can be overcome by increasing the number of grid points used in the computation at the cost of increased computer time and memory requirements. For the present calculation, 128 x 128 grid points were used, which is adequate for a study of the nature of the intensity cross spectrum at intermediate frequencies where analytical results are least reliable. For Figure 3, normalized distance of the effective phase screen from the observation point is $\zeta = 0.15$. At this distance, intensity fluctuations are fully developed for both the frequencies. It should be noted, however, that k_0, which has been used for normalization in this calculation is twice the reciprocal of the distance used for normalization by Miller [1987, equations (14) and (56)]. Consequently $\zeta = 0.15$ corresponds to a normalized distance of 0.038 in the above reference. The main difference between the present results and those obtained by Miller [1987] is that whereas in the latter, P(ν) is independent of r for low and intermediate spatial frequencies beyond the frequency at which P(ν) is maximum, Figure 3 indicates that, in the case

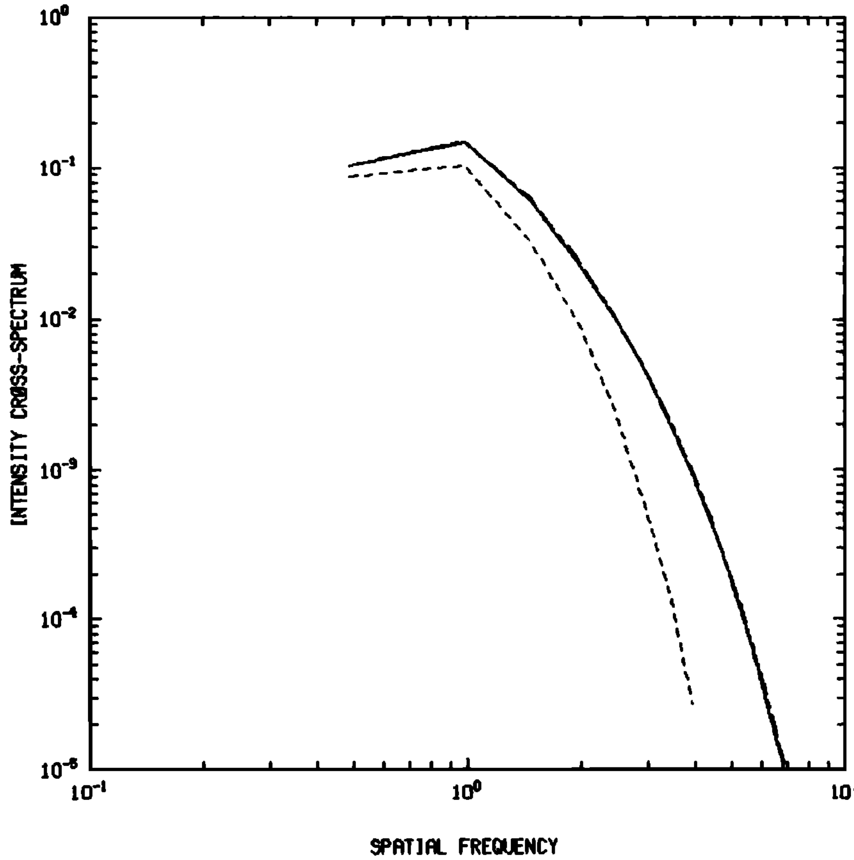

Fig. 2. Intensity cross spectra obtained with different step sizes: $\Delta\zeta = \zeta_L$ (short-dashed line); $\Delta\zeta = \zeta_L / 4$ (solid line); $\Delta\zeta = \zeta_L / 10$ (long-dashed line). The last two curves overlap. Other parameters of the irregularities are the same as for Figure 1.

under consideration here, the intensity cross-spectrum varies with r even at low spatial frequencies. This difference arises due to the nondispersive nature of the phase screen considered by Miller [1987] whereas in the present study the random medium is dispersive with a frequency dependence given by (4), a situation which pertains to radio wave propagation in the ionosphere, the interplanetary space or the interstellar medium. At high spatial frequencies, the intensity cross spectrum shows similar behavior irrespective of the wave number dependence of the refractive index of the phase screen. As demonstrated in Figure 3, the truncation of the intensity cross spectrum at high spatial frequencies occurs more rapidly with increasing deviation of r from unity, which was also observed by Uscinski and Macaskill [1985] and Miller [1987].

4. POWER LAW IRREGULARITY SPECTRUM

On the basis of experimental observations, ionospheric irregularities which cause intensity fluctuations on radio wave signals are characterized by a power law type of spectrum [Dyson et al., 1974; Umeki et al., 1977]. In particular, irregularities found in the equatorial ionosphere are usually very much elongated along the geomagnetic field direction and hence may be considered to be two-dimensional. These irregularities are frequently described by a two-dimensional power law spectrum with index 3:

$$\Phi_{\Delta N}(\vec{q}) = \frac{\langle(\Delta N)^2\rangle}{2\pi} \frac{k_0}{[k_0^2 + q^2]^{3/2}} \tag{39}$$

where $2\pi / k_0$ corresponds to the outer scale of

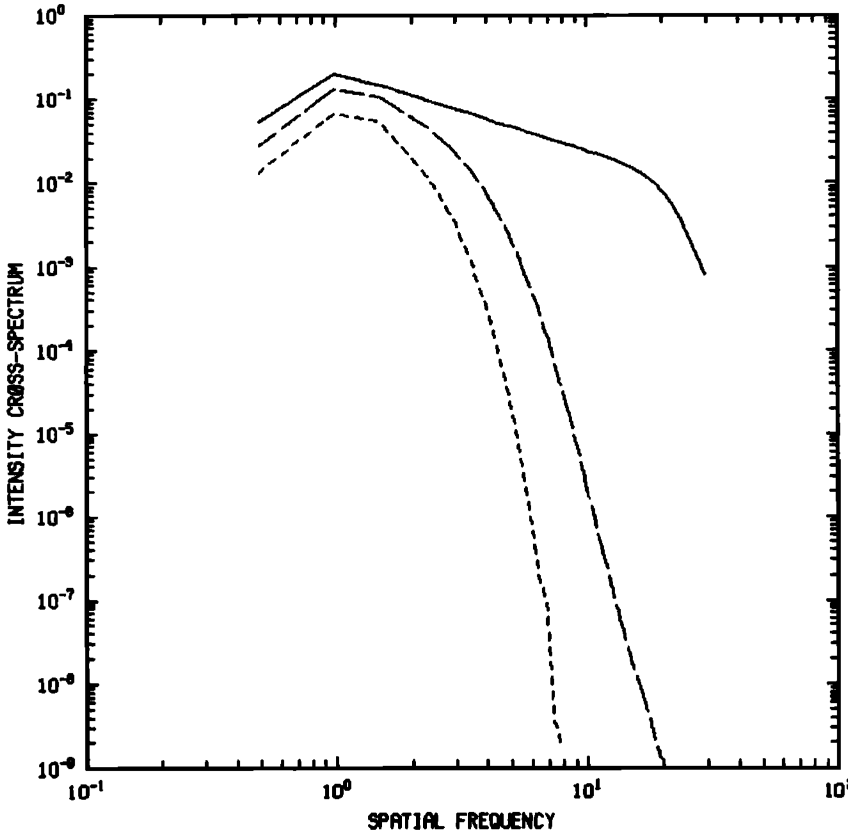

Fig. 3. Intensity cross spectra for a phase screen with Gaussian power spectrum ($\sigma_\phi^2 = 100$) for frequency ratios r = 1 (solid line); r = 0.714 (long-dashed line); r = 0.5 (short-dashed line). ζ_R = 0.15.

the irregularities. Under the assumption of frozen flow, this form of the irregularity power spectrum leads to the following expression for $F(\xi_1,\xi_2,t)$ where the explicit dependence on t has been dropped:

$$F(\xi_1,\xi_2) = 2\sigma_\phi^2\{1 + r^2 - |\xi_2|K_1(|\xi_2|)$$

$$- r^3|\xi_2|K_1(r|\xi_2|)$$

$$+ r[|\xi_1 + \frac{1+r}{2}\xi_2|K_1(|\xi_1 + \frac{1+r}{2}\xi_2|)$$

$$- |\xi_1 + \frac{1-r}{2}\xi_2|K_1(|\xi_1 + \frac{1-r}{2}\xi_2|)$$

$$- |\xi_1 - \frac{1-r}{2}\xi_2|K_1(|\xi_1 - \frac{1-r}{2}\xi_2|)$$

$$+ |\xi_1 - \frac{1+r}{2}\xi_2|K_1(|\xi_1 - \frac{1+r}{2}\xi_2|)]\} \qquad (40)$$

Here K_1 is a modified Bessel function. The normalized two-frequency intensity correlation function $R(\xi)$ and the cross spectrum $P(\nu)$ can now be computed from (37) and (38). In Figure 4, the general nature of the intensity cross spectrum is seen to be the same as found for irregularities with a Gaussian power spectrum. Uscinski and Macaskill [1985] had also reached a similar conclusion on the basis of approximate analytic expressions for the solution of the relevant fourth-moment equation. The value of σ_ϕ^2 is 56.4 for Figure 4. The normalized distance of the effective phase screen from the point of observation has been taken as $\zeta = 0.0603$, which is applicable to scintillations on a wave of frequency 125 MHz caused by irregularities at an effective height of 400 km in the ionosphere and with an outer scale ($= 2\pi/k_0$) of 10 km. For r = 1, the high-frequency asymptote of the intensity power spectrum appears to have a power law dependence of the form ν^{-p} with p = 2.55. For

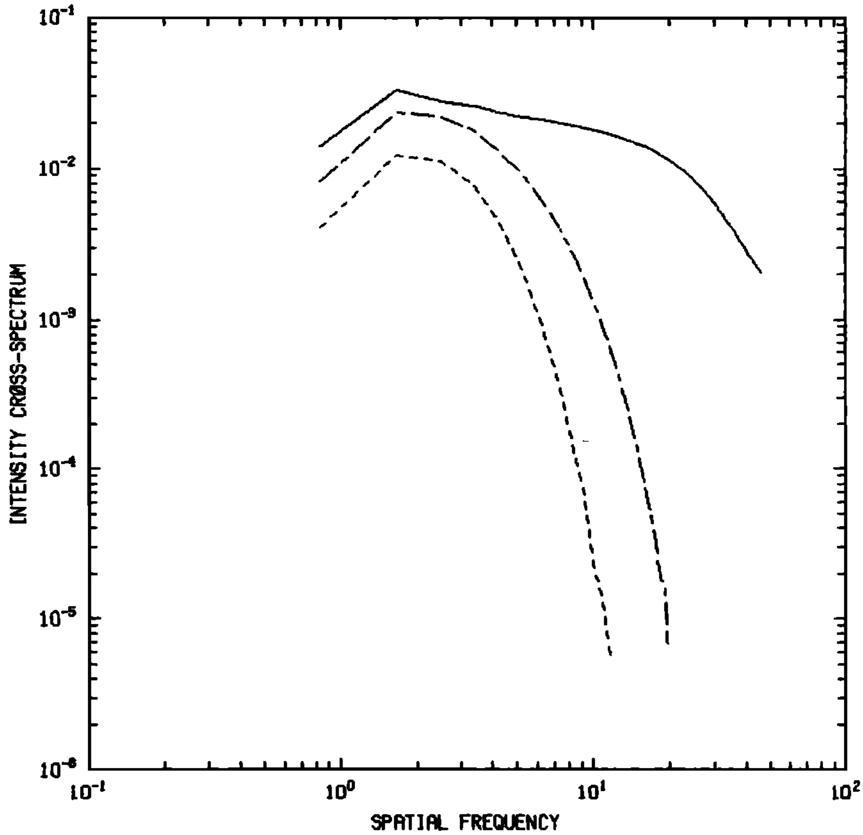

Fig. 4. Same as in Figure 3, but for irregularities with a power law spectrum with spectral index of 3, σ_ϕ^2 = 56.4, and ζ_R = 0.06.

weak intensity scintillations caused by irregularities with a two-dimensional power law spectrum with spectral index -p, the high-frequency asymptote of the intensity power spectrum has a power law dependence of the form ν^{-p} [*Yeh and Liu*, 1982]. For strong scintillations arising due to a deep phase screen, the same relationship exists between the slope of the high-frequency asymptote of the intensity power spectrum and the spectral index of the irregularity power spectrum [*Rumsey*, 1975]. The present result, which is for irregularities with a two-dimensional power law spectral index of -3 and corresponds to an S_4 index of 1.02, is in reasonable agreement with the result of *Rumsey* [1975].

In order to study the variation of the cross correlation of intensity fluctuations with the strength of the irregularities, values of

$$B_I(k_1,k_2) = R(0)/S_4(k_1)S_4(k_2) \qquad (41)$$

where $S_4(k_i)$ is the S_4 index for a signal of wave number k_i, are plotted as a function of σ_ϕ in Figure 5. The wave frequency f_1 (= $2\pi/k_1$) is taken to be 125 MHz. The center of the irregularity slab of thickness 100 km is at a height of 400 km above the receiver, and the outer scale of the irregularities is 10 km, which are the values of the parameters applicable to ionospheric propagation. In Figure 5, the two curves are for two different values of r, the ratio of the two frequencies. When $k_1 = k_2 = k$, $R(0) = S_4^2(k)$ by definition and B_I has the value 1. The normalized correlation of weak amplitude scintillations on waves of different frequencies, defined in a manner similar to $B_I(k_1,k_2)$, was shown to be independent of the strength of the irregularities in a thin phase changing screen by *Budden* [1965]. The Rytov solutions of the parabolic equations for weak scintillations due to an irregularity slab [*Yeh and Liu*, 1982] also demonstrate that in the weak scintillation limit ($\sigma_\phi^2 << 1$), B_I is independent of σ_ϕ and is

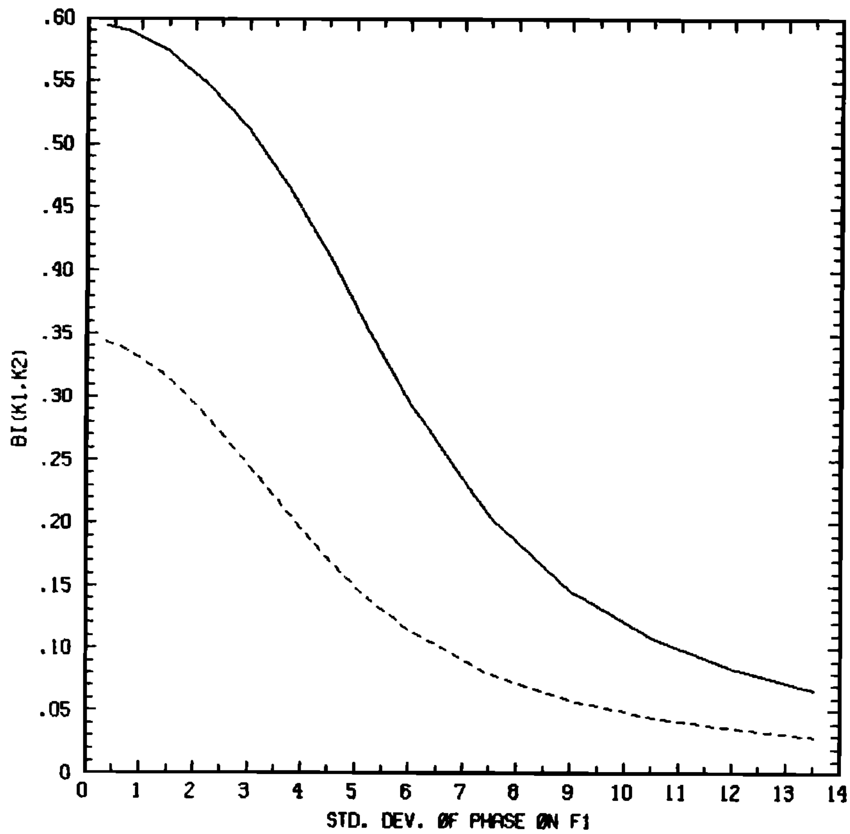

Fig. 5. Variation of the normalized intensity cross-correlation $B_I(k_1, k_2)$ (defined in (41)) with σ_ϕ for r = 0.714 (solid line) and r = 0.5 (dashed line). Irregularities have a power law spectrum with spectral index of 3. For both curves ζ_L = 0.015 and ζ_R = 0.0678.

determined by r, ζ_L and ζ_R. Whereas the analytic expression for the frequency cross spectrum of intensity fluctuations derived by Miller [1987] is valid for values of $\sigma_\phi^2 \gg 1$, the present numerical solution does not have this limitation. Thus, it is possible to investigate the dependence of $B_I(k_1,k_2)$ on σ_ϕ for a range of values of σ_ϕ starting with the weak scintillation limit. Since σ_ϕ is the standard deviation of phase fluctuations for the wave with wave number k_1, and for the curves in Figure 5, k_1 is held constant along with the height and thickness of the irregularity slab, variations in σ_ϕ are equivalent to changes in the strength of the irregularities. It is seen from Figure 5 that in the weak scintillation limit, $B_I(k_1,k_2)$ approaches a constant value determined by $r = k_1/k_2$. As the strength of the irregularities increases, the higher-frequency wave may still be considered to be singly scattered while the lower-frequency wave undergoes multiple scatterings. This results in increasing decorrelation of the intensity fluctuations on the two waves. When both the waves undergo strong scintillations, there is little further loss of correlation with increasing strength of the irregularities.

5. NONFROZEN FLOW

Temporal evolution of the irregularities in the random medium may occur due to decay caused by fluctuations in the convection velocity of the irregularities. This mechanism was considered by Shkarofsky [1968] among other mechanisms, for which he suggested that the Fourier transform $S_{\Delta N}(\vec{q},\omega)$ of the irregularity space-time correlation function $B_{\Delta N}(x,z,t)$ may be decomposed as follows:

$$S_{\Delta N}(\vec{q},\omega) = \Phi_{\Delta N}(\vec{q})\,\psi(\vec{q},\omega) \tag{42}$$

where $\Phi_{\Delta N}(\vec{q})$ is the irregularity power spectrum for frozen flow. The Fourier transform of $\psi(\vec{q},\omega)$ with respect to ω is given by

$$\psi(\vec{q},t) = \exp(-i\vec{q}\cdot\vec{v}_0 t - q^2\sigma_v^2 t^2/2) \quad (43)$$

when the decay is caused by fluctuations in the velocity of the irregularities [Shkarofsky, 1968]. Here $\vec{v}_0$ is the average drift velocity of the irregularities and σ_v is the standard deviation of the velocity fluctuations. The integrated space-time correlation function $A_{\Delta N}(x,t)$ is related to the irregularity power spectrum $S_{\Delta N}(\vec{q},t)$ through

$$A_{\Delta N}(x,t) = 2\pi \int_{-\infty}^{\infty} S_{\Delta N}(q_x,q_z = 0,t)\exp(iq\,x)\,dq_x \quad (44)$$

With the choice of the Gaussian form given in (35) for $\Phi_{\Delta N}(\vec{q})$, the following expression is derived for $F(\xi_1,\xi_2,t)$ when the irregularities have random velocity fluctuations superimposed on an uniform convection in the x direction:

$$\begin{aligned}F(\xi_1\,\xi_2,t) = 2\sigma_\phi^2\{&1+r^2 - \exp(-\xi_2^2/4) - r^2\exp(-r^2\xi_2^2/4) + \frac{r}{\alpha}\\ &\cdot(\exp[-(\xi_1 + \tfrac{1+r}{2}\xi_2 - k_0v_0t)^2/4\alpha^2]\\ &- \exp[-(\xi_1 + \tfrac{1-r}{2}\xi_2 - k_0v_0t)^2/4\alpha^2]\\ &- \exp[-(\xi_1 - \tfrac{1-r}{2}\xi_2 - k_0v_0t)^2/4\alpha^2]\\ &+ \exp[-(\xi_1 - \tfrac{1+r}{2}\xi_2 - k_0v_0t)^2/4\alpha^2])\}\end{aligned} \quad (45)$$

where

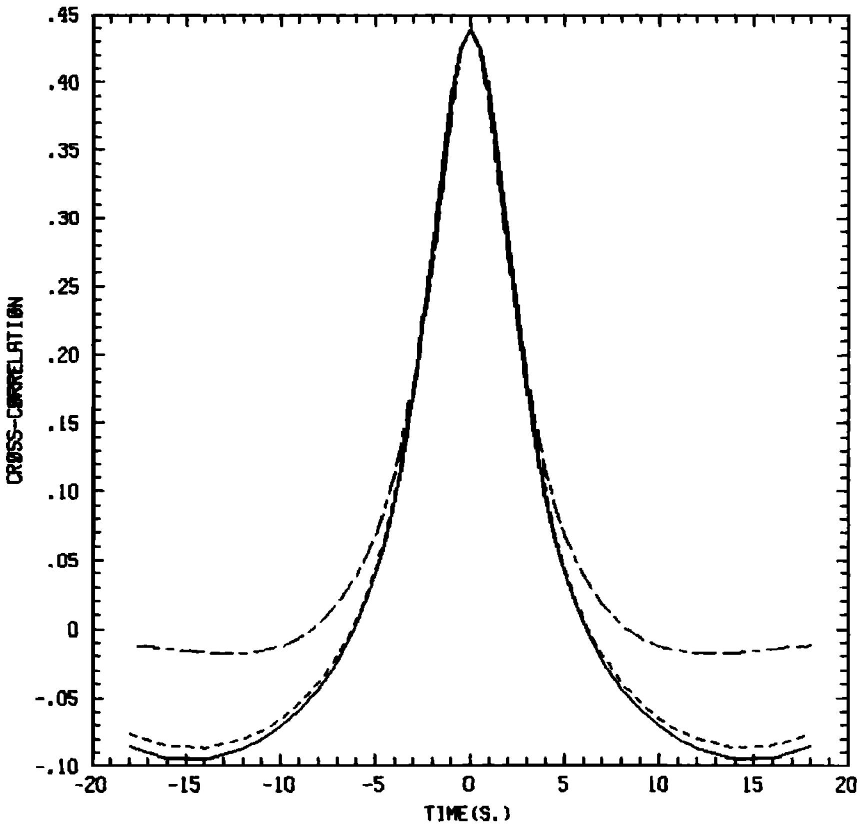

Fig. 6. Time variation of the intensity cross correlation for two frequencies with ratio r = 0.833 measured at the same location, for $\sigma_v = 0$ (solid line); $\sigma_v = 0.2\,v_0$ (short-dashed line); and $\sigma_v = 0.8\,v_0$ (long-dashed line). Irregularities have a Gaussian power spectrum with scale size $L_0 = 2$ km, $\sigma_\phi^2 = 100$ and $v_0 = 100$m/s. Here $\zeta_L = 0.019$ and $\zeta_R = 0.0668$.

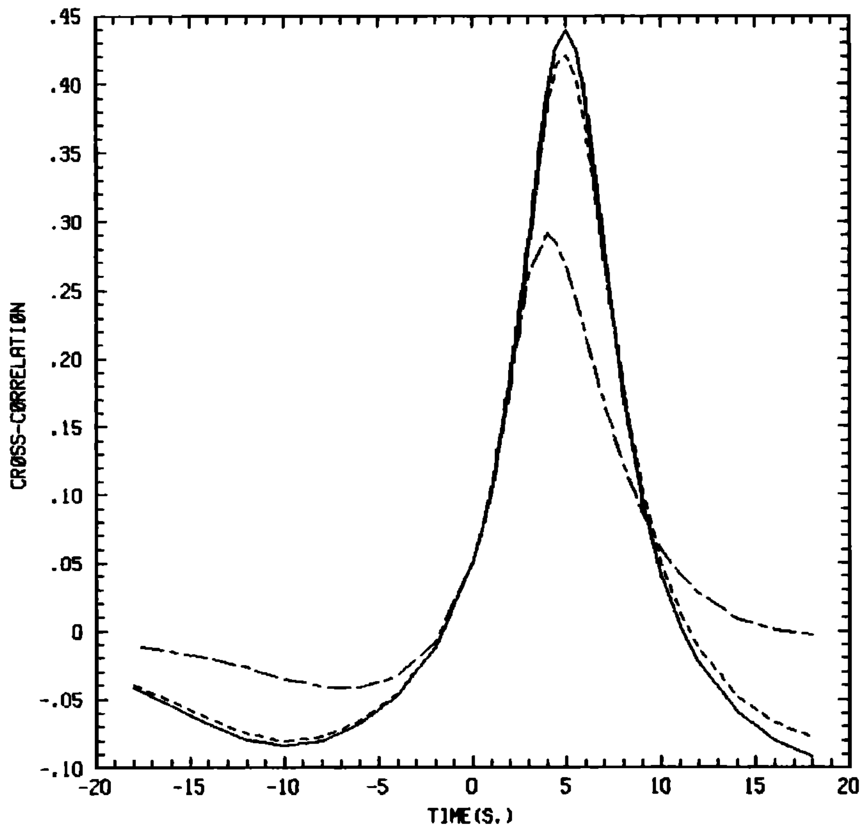

Fig. 7. Time variation of the intensity cross correlation for a spatial separation of $L_0/4$, $r = 0.833$. Here $\sigma_v = 0$ (solid line); $\sigma_v = 0.2\, v_0$ (short-dashed line); $\sigma_v = 0.8\, v_0$ (long-dashed line). Irregularity parameters are the same as in Figure 6.

$$\alpha = \left(1 + \frac{k_0^2 \sigma_v^2 t^2}{2}\right)^{1/2} \qquad (46)$$

This expression has been used to calculate $R(\xi,t)$ for several values of σ_v keeping v_0 constant. Some typical results for $\sigma_\phi^2 = 100$, when multiple scatterings take place for the wave number k_1, are shown in Figures 6, 7, and 8. For these figures, $L_0 = 2$ km, $v_0 = 100$ m/s, $f_1 = 250$ MHz, $\zeta_L = 0.019$ and $\zeta_R = 0.0668$. These values of ζ_L and ζ_R correspond to an irregularity slab of thickness 100 km at an average height of 350 km above the observation point. The cross correlation $R(0,t)$ of intensity fluctuations, observed at the same location, on two frequencies with a ratio $r = 0.833$, is depicted in Figure 6. The effect of velocity fluctuations in this case is similar to that observed in the monochromatic case [Wernik et al., 1983]; i.e., the velocity fluctuations only affect the wings of the cross-correlation function $R(0,t)$. However, when the two waves are observed at different locations, the effect of velocity fluctuations on the intensity cross-correlation function $R(\xi,t)$ is more pronounced. This can be perceived from Figure 7, where $R(\xi,t)$ for a normalized separation $\xi = 0.5$, which corresponds to a transverse distance of a quarter of the irregularity scale size, is plotted as a function of time. As the ratio σ_v/v_0 is increased from 0 to 0.8, there is an appreciable decrease in the peak value of the cross correlation. The peak also shifts toward a smaller time lag as in the monochromatic case [Wernik et al., 1983; Franke and Liu, 1987]. In addition to these effects, velocity fluctuations introduce a positive skewness in the cross-correlation function which increases with increasing σ_v, as observed in Figure 7. A comparison of Figure 7 with Figure 8, where $R(\xi = 0.5,t)$ is plotted as a function of

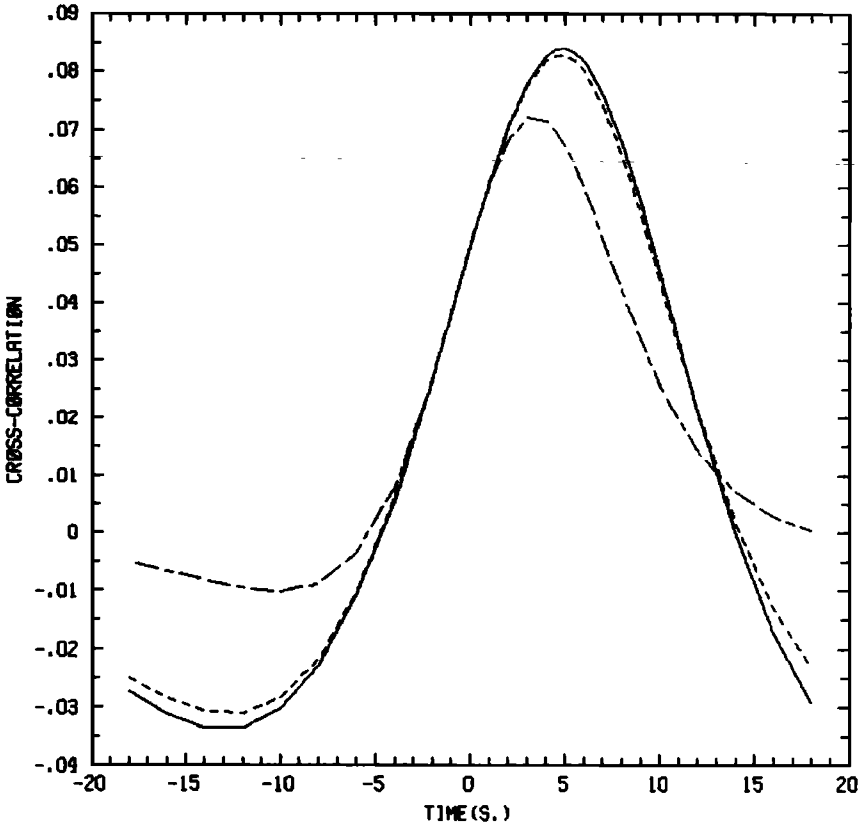

Fig. 8. Same as in Figure 7 for r = 0.5.

time for r = 0.5, shows that whereas the peak of the correlation function is broadened as the deviation of r from unity increases, the peak itself moves to a smaller time lag. Also, decorrelation associated with the velocity fluctuations decreases as r decreases. Thus velocity fluctuations cause maximum decorrelation in the case of monochromatic waves. This follows from (45), which shows that for a fixed strength of the irregularities, the σ_v - dependent terms in $F(\xi_1,\xi_2,t)$ decrease in importance as r decreases from unity.

The effect of nonfrozen flow in the case of irregularities with a power law spectrum is investigated by considering $\Phi_{\Delta N}(\vec{q})$ to be of the form

$$\Phi_{\Delta N}(\vec{q}) = \frac{<(\Delta N)^2>}{\pi} \frac{k_0^2}{[k_0^2+q^2]^2} \quad (47)$$

where $2\pi/k_0$ (= L_0) is the outer scale of the irregularities. For this form of $\Phi_{\Delta N}(\vec{q})$, it is possible to obtain an analytic expression for $F(\xi_1,\xi_2,t)$. The resultant space-time correlation function $R(\xi,t)$ for a spatial separation of $L_0/32$, where L_0 = 10 km, is shown as a function of time in Figure 9. The ratio of the two wave frequencies, σ_ϕ^2, and v_0 have the same values as in Figure 7; however, $\zeta_L = 0.0075$ and $\zeta_R = 0.033$ on account of the different value of L_0. The only difference between $R(\xi,t)$ for power law and Gaussian irregularity spectra is that in the former case, the skewness of the cross-correlation function for a fixed spatial separation, caused by the velocity fluctuations, is more pronounced than in the latter case.

6. CONCLUSION

The fourth-moment equation with different wave numbers is solved numerically using a split step algorithm which replaces the extended random medium by a series of phase screens interspersed with diffraction layers. The

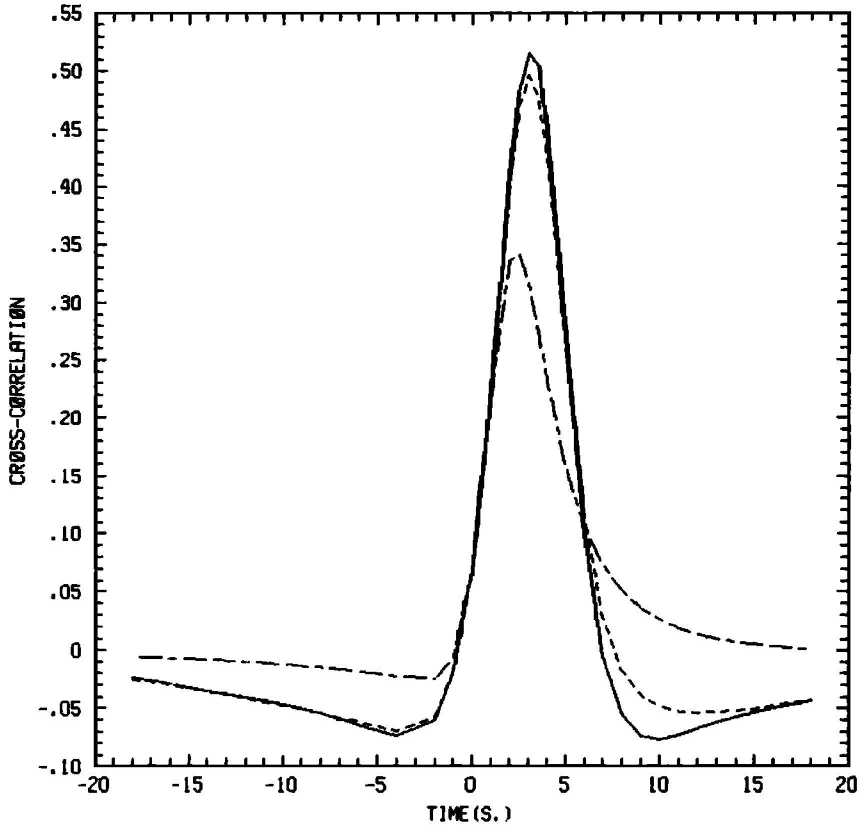

Fig. 9. Time variation of the intensity cross correlation for a spatial separation of $L_0 / 32$ in the case of a power law irregularity spectrum with spectral index 4 and outer scale L_0 = 10 km. Here r = 0.833, σ_ϕ^2 = 100, ζ_L = 0.0075, ζ_R = 0.033 and v_0 = 100 m/s. The three curves are as follows: σ_v = 0 (solid line), σ_v = 0.2 v_0 (short-dashed line), and σ_v = 0.8 v_0 (long-dashed line).

following results are obtained: (1) The spatial correlation function for intensity fluctuations due to irregularities in an extended random medium is compared with the correlation function obtained for a centrally located phase screen, under the assumption of "frozen flow." The two results differ significantly as the thickness of the irregularity slab is increased because propagation within the slab becomes important on account of additional diffraction effects which arise due to the difference in the frequencies of the two waves. (2) Comparison with the analytical results obtained by Miller [1987] shows that the intensity cross spectrum has the same characteristics at high spatial frequencies irrespective of the wave number dependence of the refractive index of the medium. The intensity cross spectrum at high spatial frequencies decreases more rapidly as the ratio of the two wave frequencies deviates from unity. On the other hand, for low frequencies, the nature of the intensity cross spectrum is determined by the wave number dependence of the refractive index fluctuations. (3) The general behavior of the intensity cross spectrum remains unchanged when the irregularities have a power law spectrum instead of a Gaussian spectrum. (4) Multiple scatterings on the lower-frequency wave cause further decorrelation of intensity fluctuations on the two waves as the strength of the irregularities is increased. (5) The two-frequency space-time intensity correlation function is obtained for the "nonfrozen" situation where the irregularities have random velocity fluctuations with standard deviation σ_v superimposed on a uniform drift. The effects produced by the velocity fluctuations are similar to those in the monochromatic case [Wernik et al., 1983; Franke and Liu, 1987]. The peak value of the cross-correlation function for different spatial locations decreases as σ_V increases and the peak itself moves toward a smaller time lag and has a positive skewness. However, velocity fluctuations become increasingly ineffective in causing decorrelation as the ratio of the two frequencies deviates from unity.

It has been demonstrated by Uscinski [1985] that for monochromatic plane waves which undergo multiple scattering, the multiple convolution solution is equivalent to the field of a wave that has traversed $N(= 2\sigma_\phi^2 >> 1)$ phase screens, each of which gives rise to a mean square phase deviation of 0.5 (rad)^2 and is located at a distance L/N from the next phase screen. This equivalence should also hold for a multiple convolution solution of the fourth-moment equation for waves of two different frequencies obtained by Uscinski and Macaskill [1985]. Thus, in principle, the split step solution obtained in the present study would yield the same result as the multiple convolution solution, if the number of steps within the random medium is taken to be equal to $2\sigma_\phi^2$ when $\sigma_\phi >> 1$. However, on the basis of the numerical results obtained here, it is found that, in practice, the split step solution for the two-frequency intensity space-time correlation function converges rapidly as the number of steps within the random medium is increased, and therefore, the number of steps required for an accurate estimate of the two-frequency intensity correlation is much less than $2\sigma_\phi^2$ when $\sigma_\phi >> 1$. It may be possible to cast the multiple convolution solution in a form where this convergence can be demonstrated analytically, in which case the split step scheme of solving the fourth-moment equation could provide a practical means of evaluating the multiple convolution solution.

Acknowledgments. This research was partially supported by the National Science Foundation under grant ATM 84 14134. We would like to thank S. J. Franke for a number of discussions and suggestions.

REFERENCES

Booker, H. G., J. A. Ferguson, and H. O. Vats, Comparison between the extended medium and the phase-screen scintillation theories, J. Atmos. Terr. Phys., 47, 381-399, 1985.

Budden, K. G., The theory of the correlation of amplitude fluctuations of radio signals at two frequencies, simultaneously scattered by the ionosphere, J. Atmos. Terr. Phys., 27, 883-897, 1965.

DiNapoli, F. R., and R. L. Deavenport, Topics in current physics, in Ocean Acoustics, edited by J. A. DeSanto, chap. 3, Springer-Verlag, New York, 1979.

Dyson, P. L., J. P. McClure, and W. B. Hanson, In-situ measurements of the spectral characteristics of F region ionospheric irregularities, J. Geophys. Res., 79, 1497-1502, 1974.

Franke, S. J., and C. H. Liu, Space-time statistics of waves propagating through a deep phase screen, Conf. Proc. 419, p. 15-1, Adv. Group for Aerosp. Res. and Dev., NATO, Brussels, 1987.

Lee, M. C., Wave propagation in a random medium: A complete set of the moment equations with different wave numbers, J. Math. Phys., 15, 1431-1435, 1974.

Lerche, I., Scintillations in astrophysics, I, An analytic solution of the second-order moment equation, Astrophys. J., 234, 262-274, 1979.

Liu, C. H., and K. C. Yeh, Frequency and spatial correlation functions in a fading communication channel through the ionosphere, Radio Sci., 10, 1055-1061, 1975.

Mazar, R., J. Gozani, and M. Tur, Two-scale solution for the intensity fluctuations of two-frequency wave propagation in a random medium, J. Opt. Soc. Am., A, 2, 2152-2160, 1985.

Miller, S. J., Frequency cross-spectrum of intensity fluctuations produced by a deep-phase screen, Proc. R. Soc. London, Ser. A, 410, 229-249, 1987.

Miller, S. J., and B. J. Uscinski, Frequency cross-correlation of intensity fluctuations; Limitations of multiple-scatter solutions, Opt. Acta, 33, 1341-1358, 1986.

Rino, C. L., Iterative methods for treating the multiple scattering of radio waves, J. Atmos. Terr. Phys., 40, 1011-1018, 1978.

Rumsey, V. H., Scintillations due to a concentrated layer with a power law turbulence spectrum, Radio Sci., 10, 107-114, 1975.

Shkarofsky, I. P., Turbulence functions useful for probes (space-time correlation) and for scattering (wave number-frequency-spectrum) analysis, Can. J. Phys., 46, 2683-2702, 1968.

Tur, M., Numerical solutions for the fourth moment of a finite beam propagating in a random medium, J. Opt. Soc. Am. A., 2, 2161-2170, 1985.

Umeki, R., C. H. Liu, and K. C. Yeh, Multifrequency spectra of ionospheric amplitude scintillations, J. Geophys. Res., 82, 2752-2760, 1977.

Uscinski, B. J., Analytical solution of the fourth-moment equation and interpretation as a set of phase screens, J. Opt. Soc. Am., A, 2, 2077-2091, 1985.

Uscinski, B. J., and C. Macaskill, Frequency cross-correlation of intensity fluctuations in multiple scattering, Opt. Acta, 32, 71-89, 1985.

Wagen, J.-F., and K. C. Yeh, A numerical study of waves reflected from a turbulent ionosphere, Radio Sci., 21, 583-604, 1986.

Wernik, A. W., C. H. Liu, and K. C. Yeh, Modeling of spaced-receiver scintillation measurements, Radio Sci., 18, 743-764, 1983.

Yeh, K. C., and C. H. Liu, Radio wave scintillations in the ionosphere, Proc. IEEE, 70, 324-360, 1982.

Zavorotnyi, V. U., Frequency correlation of large intensity fluctuations in a turbulent medium, Radiofizika, Engl. Transl., 24, 601-608, 1981.

A. Bhattacharyya and K. C. Yeh, Department of Electrical and Computer Engineering, University of Illinois, Urbana, IL 61801.